한국환경과학회지 제14권(제1호), 1~8, 2005
*Journal of the Environmental Sciences*

# Evaluation of a Large Space Indoor Air Flow Controling System with a CFD code for Enhancing indoor Environment

**Yong-Hyun Chung, Junji Onishi*, Haruo Soeda* and Dong-Gyu Kim****
*Division of Environmental Engineering, Pukyong National University, Busan 608-739, Korea*
**Dept. of Intelligent Machine Engineering, Osaka Electro-Communication University, Osaka 572-8530, Japan*
***Global Environmental Eng., Busan 611-070, Korea*
*(Manuscript received 8 October, 2004; accepted 13 January, 2005)*

CFD code are used for numerically testing a new concept of large space air control system. A workshop with air-conditioners products lines and air-conditioned by several floor type air-containers is tested. The whole room air distribution is controlled by boosters installed in a middle height horizontal plane. First, calculated results are compared with measured data to confirm the validity and applicability of the prediction method. Next, the method is applied to case studies heating seasons. Results under some operating conditions show effectiveness in avoid the temperature stratification in winter.

Key Words : Indoor Environment, Large space, CFD, Air flow controling system

## 1. Introduction

It has been focussed to reduce the energy consumption by introducing a suitable technologies. From this point of view, in the air-conditioning or ventilating system designs for large spaces, such as factories, atria or halls, how to realize optimum air distributions efficiently in heating or cooling seasons is one of the important issues. For example, some flow control devices such as conventional distributor systems are necessary to avoid the temperature stratification for enhancing thermal environment conditions of indoor and energy saving.

Before the CFD techniques become the useful mean for predicting flow fields in rooms, the evaluation of air-conditioning or ventilating systems depends on experimental approaches such as field measurements or model room testings, Recent advance in CFD methods may enable us to replace such experiments on numerical simulations rather successfully.

In this paper, a new concept of a large space air flow control system is evaluated. In the new system, boosters are installed in a middle height horizontal plane and they accelerate room air flows horizontally to control the whole room air distributions.

The aim of this study is to confirm the applicability of the CFD method developed by authors [SCIENCE CODE used for indoor fluid analysis][1~5] to a wide and 'thin' space with complex air outlet conditions. It also includes investigation of performance of new system applied to a large test space using the CFD code.

## 2. Numerical Method

### 2.1. Governing equations

SCIENCE CODE is based on the 3D transient fluid governing equations. The indoor airflow is treated as turbulence flow. These equations are used in the time averaged form and a standard $k-\varepsilon$ turbulence model is applied.

Continuity equation

$$\frac{\partial u_i}{\partial x_j}=0 \tag{1}$$

Momentum equation

$$\frac{\partial(\rho u_i)}{\partial t}+\frac{\partial(\rho u_j u_i)}{\partial x_j}$$

Corresponding Author : Yong-Hyun Chung, Division of Environmental Engineering, Pukyong National University, Busan 608-739, Korea
Phone: +82-51-620-6443
E-mail: chungyh@pknu.ac.kr

$$= -\frac{\partial p}{\partial x_i} + \frac{\partial}{\partial x_j}\left\{(\mu+\mu_t)\left(\frac{\partial u_i}{\partial x_j}+\frac{\partial u_j}{\partial x_i}\right)\right\} + F_i \quad (2)$$

Scalar quantity $\phi$ equation

$$\frac{\partial(\rho\phi)}{\partial t} + \frac{\partial(\rho u_j \phi)}{\partial x_j} = \frac{\partial}{\partial x_j}\left\{(\Gamma^{\phi}+\Gamma_t^{\phi})\frac{\partial \phi}{\partial x_j}\right\} + S_{\phi} \quad (3)$$

$k$-equation

$$\frac{\partial(\rho k)}{\partial t} + \frac{\partial(\rho u_j k)}{\partial x_j} = \frac{\partial}{\partial x_j}\left\{\left(\mu+\frac{\mu_t}{\sigma_k}\right)\frac{\partial k}{\partial x_j}\right\} + G + B - \rho\varepsilon \quad (4)$$

$\varepsilon$-equation

$$\frac{\partial(\rho\varepsilon)}{\partial t} + \frac{\partial(\rho u_j \varepsilon)}{\partial x_j} = \frac{\partial}{\partial x_j}\left\{\left(\mu+\frac{\mu_t}{\sigma_\varepsilon}\right)\frac{\partial \varepsilon}{\partial x_j}\right\} + C_1\frac{k}{\varepsilon}(G+B) - C_2\rho\frac{\varepsilon^2}{k} \quad (5)$$

where, $\rho$ denotes the solution density, $F_i$ denotes the body force in the $i$ direction and $S_\phi$ denotes the source term concerned with the scalar quantity $\phi$. The notation, "-" that means time- averaged is omitted.

$G$ and $B$ that are the source term and the buoyancy term of turbulent energy $k$, are expressed as the following equation respectively,

$$G = \mu_t \frac{\partial u_i}{\partial x_i}\left(\frac{\partial u_i}{\partial x_j}+\frac{\partial u_j}{\partial x_i}\right) \quad (6)$$

$$B = gB\frac{\mu_t}{\sigma_t}\frac{\partial T}{\partial x_j} \quad (7)$$

$C_D$, $C_1$, $C_2$, $\sigma_k$ and $\sigma_\varepsilon$ expressed in the above equations are all of the experiential constants of $k-\varepsilon$ two-equation model that were recommended by Launder and Spalding[6].

The eddy viscosity $\mu_t$is defined as

$$\mu_t = C_D\frac{\rho k^2}{\varepsilon} \quad (8)$$

2.2. Numerical procedure

Basic equations for incompressible non-isothermal flows are descretized using the finite difference method and solved by SIMPLE algorithm[7]with power law scheme. As a turbulence model, ordinary κ-ε two equation model is adopted. As shown in Fig. I, the product line and other solid bodies inside the space are expressed by calculation cells as exact as possible. In

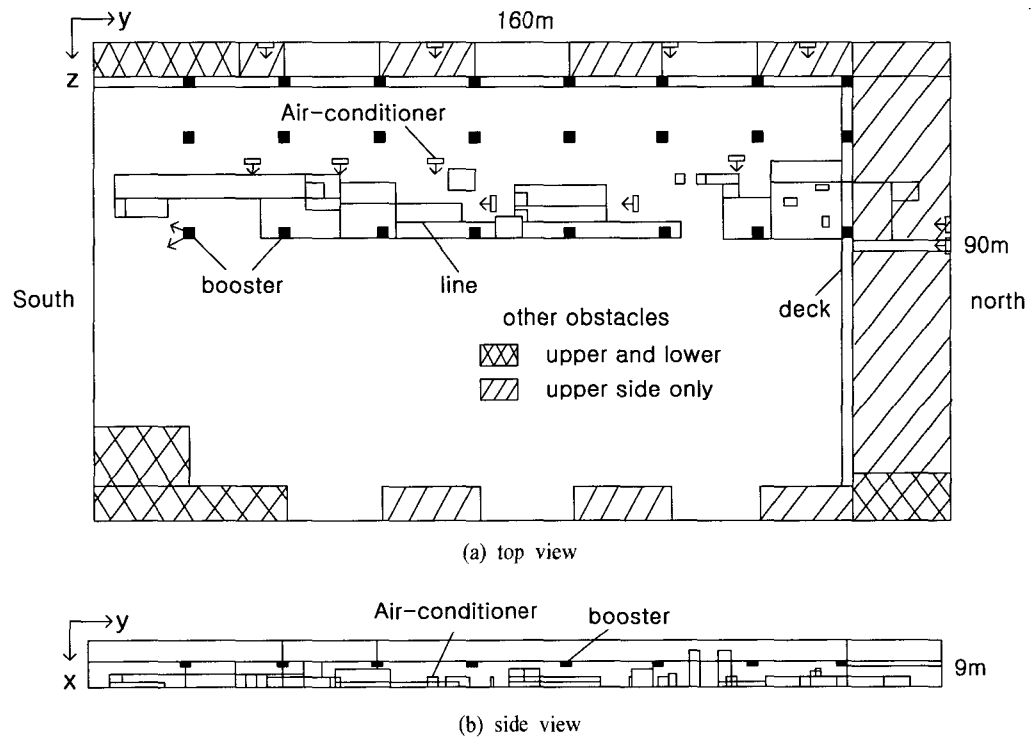


Fig. 1. Room configuration.

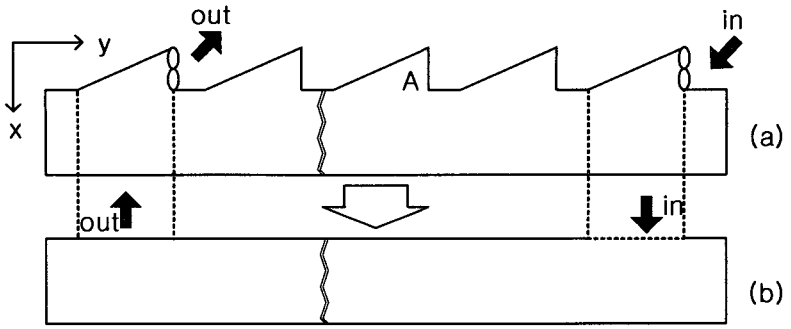


Fig. 2. Simplification of roof.

Table 1. Calculating conditions

| | $\theta_{in}$[℃] | $V_{in}$[m/s] | $\theta_{oa}$[℃] | $v_{bj}$[m/s] | weather |
|---|---|---|---|---|---|
| summer | 12.7 | 8.0 | 26.6 | 7.1 | cloudy |
| winter | 44.0 | 8.0 | 9.0 | 7.1 | cloudy |

constructing non-uniform mesh system, the ratio of neighboring mesh $r=\triangle x_{i+1}/\triangle x_i$ is set less than 1.4 to avoid increasing truncation error caused by non- uniformity of the meshes. The calculation mesh size is 20×113×56. The maximum and minimum sizes of each coordinate are $\triangle x_{max}$=1.0m, $\triangle x_{min}$=0.26m, $\triangle y_{max}$=3.0m, $\triangle y_{min}$=0.5m and $\triangle z_{max}$= 3m, $\triangle z_{min}$=0.5m respectively.

As measured velocity profiles of booster jets are very sharp(maximum velocity is about 16m/s), very fine meshes are necessary to express them exactly. Then, in the calculation model, each nozzle jet is expressed with two meshes and set uniform velocity so as to be equal the modeled jet momentum to measured jet momentum. Such approximation may be not acceptable in analyzing the jet itself or small room air flows, but in simulating large space air movement like the present study, it may not affect the result seriously except small regions adjacent to the jet.

In the actual space, ventilating air is supplied by roof mounted fans as shown in Fig. 2(a). However, because the supplied fresh air spreads widely and flow downward slowly (about 0.1m/s) and moreover the area shown in Fig. 2(a) 'A' may be regarded as dead flow zone, therefore, the roof shown in Fig. 2(a) is teated as a flat roof shown in Fig. 2(b) in the calculation model.

The ventilation rate n = V/Q is set unity in the standard case, V is space capacity($m^3$) and Q is supply outer air flow rate ($m^3$/h).

As the wall boundary condition of velocity components u, v and w, 'slip value' is given assuming power law distributions near wall surfaces. For k and ε, no slip condition is assumed.

In the calculation of temperature, walls are included inside calculation domain and sol-air temperatures are used as the boundary conditions at outer surface of walls. One mesh is given to express 'virtual wall' the thickness of which is equal to fluid cell adjacent to the wall. It's equivalent heat conductivity $\lambda_{eq}$ is so determined that its thermal resistance is equal to that of the real wall. At the inner surface (i.e. at the wall-fluid interface) heat conductivity $\lambda_{int}$ is given by harmonic mean of $\lambda_{eq}$ and $\lambda_{eff}$. The effective conductivity $\lambda_{eff}$ is estimated using empirical data of convective heat transfer efficient for room air flows[8].

2.3. Calculating conditions

Calculating conditions are shown in Table 1.

$\theta_{in}$ and $V_{in}$ are supply air temperature and velocity of air-conditioner. $\theta_{oa}$ is outer air temperature. $V_{bj}$ is booster jet velocity respectively.

Sol-air temperatures are shown in Table 2 together with thermal conductance of each wall. All data for summer are based upon measurements, but those for winter are assumed ones.

2.4 Details of the system

Details of the test space is shown in Fig. 1. It is a factory with a air-conditioner product line and it's dimensions are 160m×90m×9m respectively. It is air-conditioned by 12 floor type air-conditioners per line

Table 2. Boundary condition of temperature

| Wall Position | $K_w$ [W/m$^2$ · K] | θsa(winter) [℃] | θsa(summer) [℃] |
|---|---|---|---|
| east(wall) | 1.75 | 28.5 | 10.1 |
| east(glass) | 130 | 31.3 | 11.6 |
| west(wall) | 1.75 | 31.1 | 11.8 |
| west(glass) | 130 | 37.6 | 15.9 |
| south(wall) | 1.75 | 29.1 | 11.5 |
| south(glass) | 130 | 32.7 | 15.2 |
| north(lower) | 1.75 | 28.5 | 10.1 |
| north(upper) | insulated | - | - |
| roof | 0.46 | 33.2 | 12.2 |
| floor | insulated | - | - |

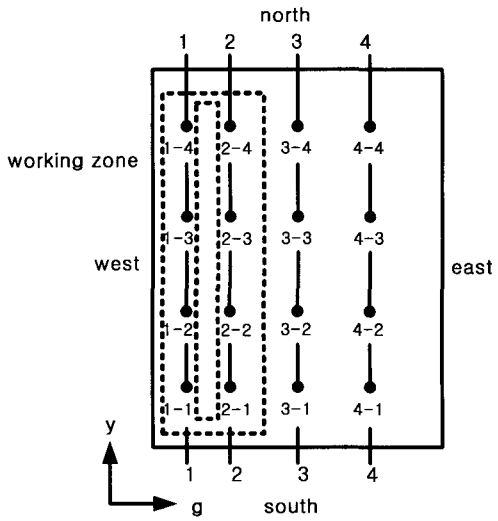


Fig. 3. Position plot.

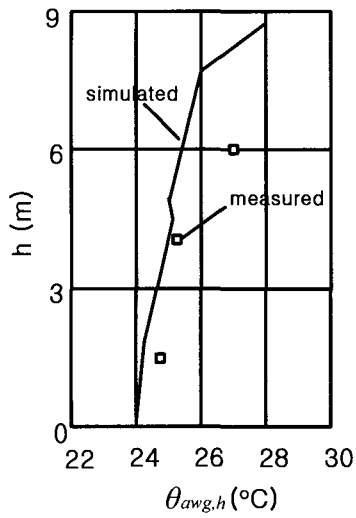


Fig. 4. Vertical change of $\theta_{avg,h}$.

and the whole room air distribution is controlled by boosters installed in a horizontal plane the height of which is about 2m higher than the working zone. Small arrows in Fig. 1 indicate the supply air directions of the air-conditioners. Each booster has a fan and two nozzles the diameter of which is 150mm. Each nozzle is set about ±45°inclined to the y-axis and discharges room air horizontally. The fresh air is supplied with axial flow fans mounted on the roof and exhausted with fans mounted on the other side of It (Fig. 2(a)).

## 3. Results and Discussion

All calculations are executed using SOR, but are very unstable, especially at initial iterations, so the relaxation parameters should be set less than 0.1 for velocities and turbulent parameters. In the present study, two factors may influence the calculation stability. One is that calculation cells with relatively large aspect ratio are included and the other is that there are many air-outlets in the calculation domain which make the flow field very complex In this study, the room is very wide and thin and moreover finer meshes should be used to express air-conditioner or boosters, it is unavoidable to use large aspect-ratio cells if ordinary mesh system is adopted. One of the remedy may be to apply locally mesh refinement (LMR) technique[9].

Fig. 4-7 presents the comparison of simulated results with measured data in summer. Velocity and temperature are measured with hot wire anemometer (KANOMAX Model 6511) at 103 points in three horizontal plane.

Vertical temperature distributions are shown in Fig. 4-5. $\theta_{avg,h}$ is the averaged temperature in the horizontal plane, h is the distance from the floor.

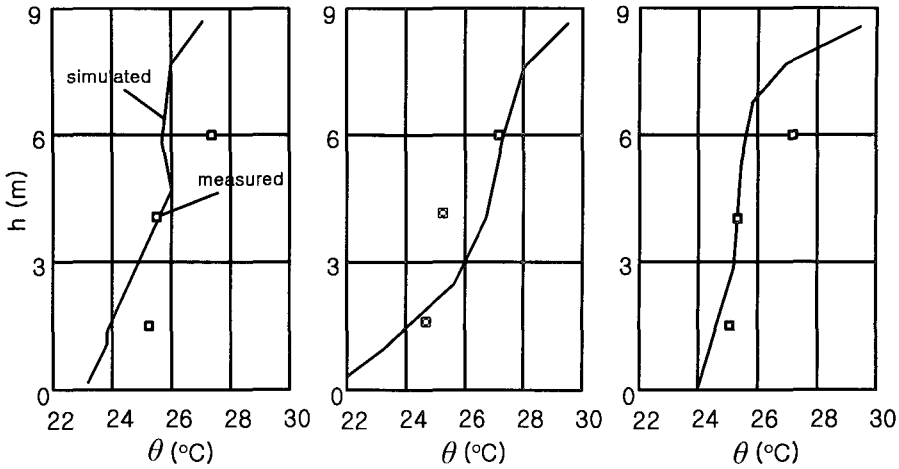


a) position 1-2 b) position 1-4 c) position 2-3

Fig. 5. Vertical distribution of temperature.

It may be read in Fig. 4 that (1) temperature increases gradually from the floor to the ceiling, (2) in the upper zone, simulated temperature is lower than measured ones (3) in the working zone ($0 \leq h \leq 2m$) averaged temperature is about 24℃.

In the simulation, infiltrations are not considered although some amount of outer air infiltrates into the space from side walls. This may be one of the causes of (2) what is described above.

In the view of quantity of measured datum and simulation results, In Fig. 6, velocity and temperature distributions (h=1.5m) are compared along line 1-1(Fig. 3) as dimensionless forms.

Where, $\upsilon^*_{yz} = \upsilon_{yz} / V_{in}$ , $\theta^* = (\theta - \theta_{in})/(\theta_{sa,max} - \theta_{in})$, $y^* = y/L$ and $v_{yz} = \sqrt{v^2 + w^2}$, $\theta_{sa,max}$ is maximum sol-air temperature shown in Table 1, L is room width (=160m). In case 1, the same mesh system used in the calculation shown in Fig. 4, 5 is used, while in case 2 LMR method is applied to boosters (the meshes expressing them are two times finer than those of case-1) and resulting $V_{bj}$ is 10m/s.

Inspection of results shown in Fig. 6 indicates that both velocity and temperature distributions gives a little sharper peak in case-2 than in case-1 because of the sharper jet velocity distributions. However, as the momentum of booster jets are set equal in both cases, both results show similar tendency and are same order in accuracy. From all results here, the maximum discrepancy between measurements and simulations is within 5% in dimensionless values.

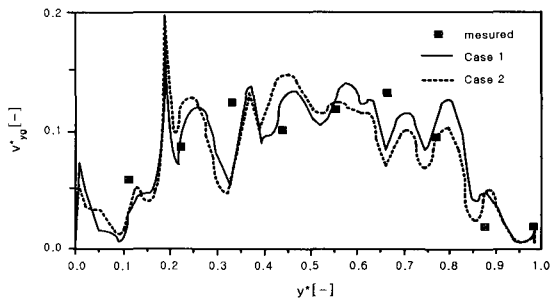


(a) Scalar velocity

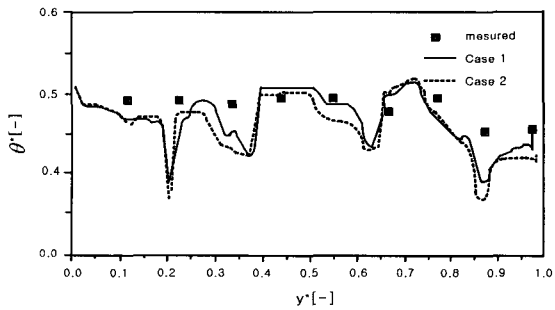


(b) Temperature

Fig. 6. Velocity and temperature distributions along line 1-1.

As an example of flow field, velocity vector distributions are given in Fig. 7 together with the measured flow directions in h=1.5m, h=4m, h=6m plane. In the view of qualitative side, it meets measured datum and results of simulation in each case.

Finally, simulation of some cases including the booster jets system is conducted to overcome stratification of the test space in heating season. Simulation

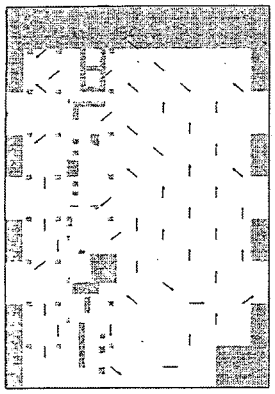

a) Flow direction (h=6m)

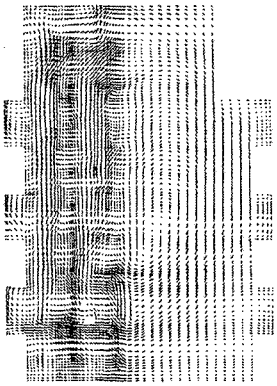

a) Velocity vectors of case1

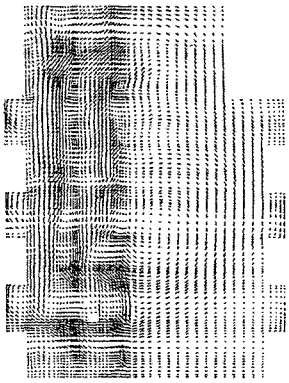

a) Velocity vectors of case2

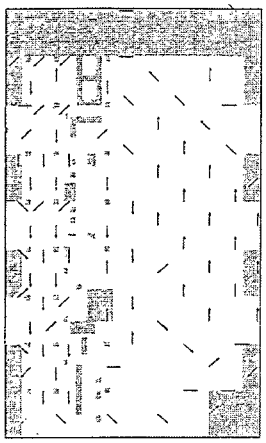

b) Flow direction (h=4m)

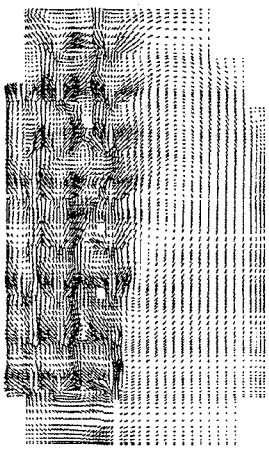

b) Velocity vectors of case1

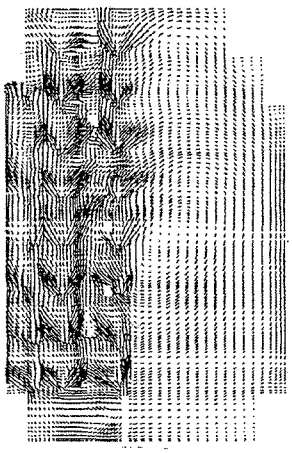

b) Velocity vectors of case2

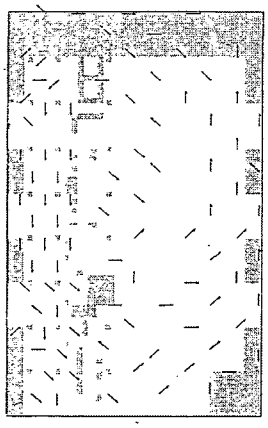

c) Flow direction (h=1.5m)

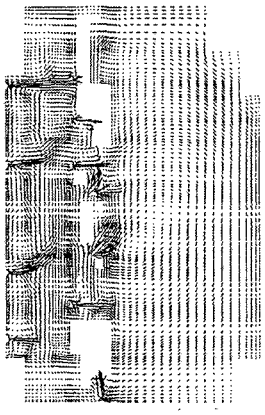

c) Velocity vectors of case1

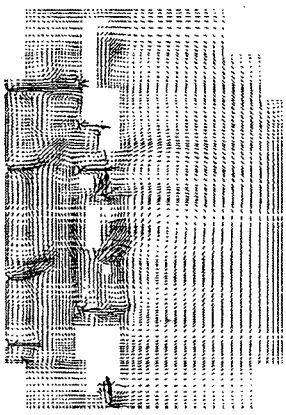

c) Velocity vectors of case2

Fig. 7. Flow directions and velocity vector(y-z plane).

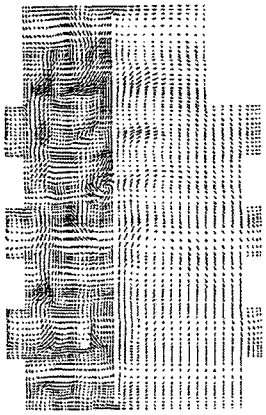

a) Velocity vectors at h=6m

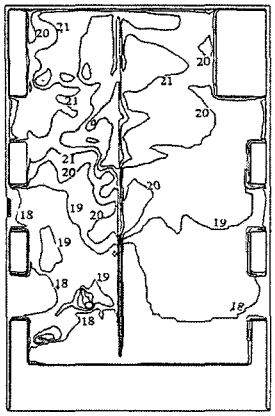

a) Temp. distribution at h=6m

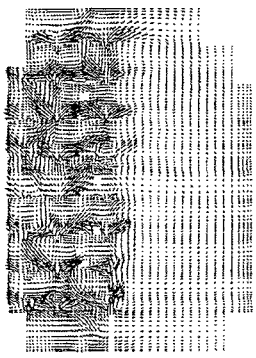

b) Velocity vectors at h=4m

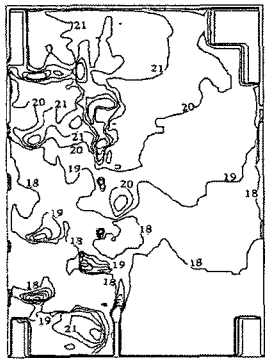

b) Temp. distribution at h=4m

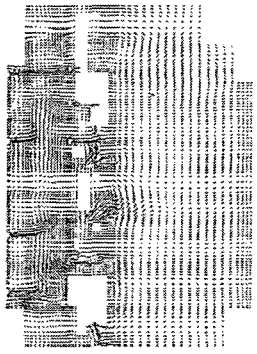

a) Velocity vectors at h=1.5m

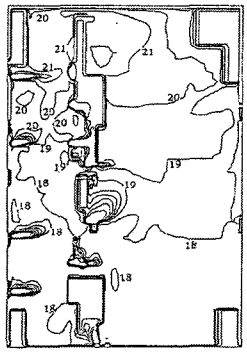

c) Temp. distribution at h=1.5m

Fig. 8. Velocity vectors and temperature distributions each height of case 3.

conditions of each case is as follows.

case-1 : same conditions as summer except weather

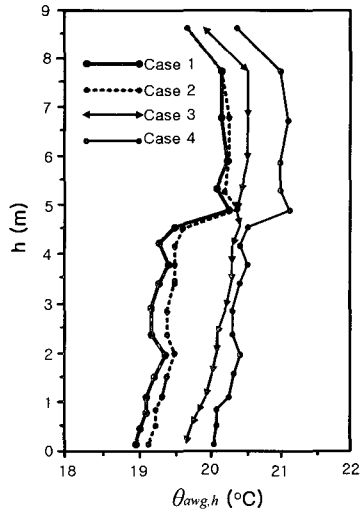


Fig. 9. Vertical distribution of temperature.

data, case-2:same as case-1 except n is set 0.5 to reduce the heating load, case-3 : booster jets are discharged to west(z-direction) and others are same as case-2, case-4 : in the middle plane between east and west wall, a vertical 'curtain'(4m height) is set from the ceiling to restrict z-directional air flows and others are same as case-1.

Only case-3 of the simulation of velocity vectors and temperature distributions are shown in Fig. 8. Fig. 9 is plots of vertical change of horizontally averaged temperature $\theta_{avg,h}$ from Fig. 8 including the data not shown here. From the results, case 3 indicates that the heated air is not staying around the ceiling. The effect of the vertical curtain is not recognized, however the change of booster jets direction is effective in decreasing the temperature stratification.

## 4. Conclusions

In the numerical investigation of a large space flow control system, following facts are clarified. In the CFD simulations of a large space with complex fields, calculations were significantly unstable. How to improve the stability and minimize the computer effort is one of the important issues. Proven by the validity of the simulations and usefulness of the CFD method adopted here. The new concept introduced in this study may be useful means in large space air flow controls.

1) From the results, comparisons with measured data shown the maximum discrepancy between measure-

ments and simulations is within 5% in dimensionless values on both velocity and temperature distributions.

2) To decrease the temperature stratification, The change of booster jets direction is more effective than the vertical curtain from the point of vertical change of horizontally averaged temperature.

However, to find the optimum operating conditions of the system, more investigation is necessary including thermal comfort analyses and/or contaminant control analyses. In those situation, the numerical simulations with CFD method may be indispensable means.

## Acknowledgements

This research was conducted as invited-researcher and supported by Osaka Electro-Communication University.

## References

1) Onishi, J., H. Soeda, S. Nakamura, K. Mori, Y. H. Chung and H. Kimoto, 2002, Development of numerical method for estimation of energy consumption in various residential houses including passive solar ones, in Proceedings of EuroSun2002 Scientific-Technical congress & Ploicy Forum on Renewable Energy for Local Communities of Europe(Toward Rio +10), ISES, bologna, paper76.

2) Onishi, J., H. Soeda and M. Mizuno, 2000, Numerical Study on a Low Energy Architecture based upon Distributed heat storage system, Renewable energy, 22, 61-66.

3) Onishi, J. and S. Tanaka, 1990, Applicability and limitations of a numerical method in thermal environment analysis for air-conditioned rooms, in Proceedings of the Room-Vent '90, A1-6, 1-15.

4) Onishi, J., S. Koga, M. Mizuno, N. Takeya and K. Kitagawa, 1998, Computer Effort saving Methods in Unsteady Calculations of Room Airflows and Thermal Environments, in Proceedings of the Room-Vent '98 6th International Conference on Air Distribution in Rooms, Stockholm, 117-123pp.

5) Onishi, J., N. Takeya and M. Mizuno, 1995, Study on numerical prediction methods for indoor airflow and thermal environments(Part 1), Transactions of SHASEJ, 55, 23-34.

6) Launder, B. E. and D. B. Spalding, 1972, Mathematical Models of Turbulence, Academic Press, London, 269pp.

7) Patankar, S. V., 1980, Numerical Heat Transfer and Fluid Flow, McGraw-Hill, 130pp.

8) Onishi, J., S. Tanaka and M. Naito, 1988, Numerical Prediction of Room Air Distributins- Effects of calculation procedures at Fluid-Solid interfaces, in Proceedings of the ASHRAE symposium on Building systems, Illinois, 161-168pp.

9) Ishida, H. and J. Onishi, 1993, Study on Enhanced Calculation using Locally Mesh Refinement with SIMPLE method, in Proceedings of 7th CFD symposium, Tokyo, 475-478pp.